IJRCS

International Journal of Robotics and Control Systems
Vol. 3, No. 1, 2023, pp. 120-133
ISSN 2775-2658
http://pubs2.ascee.org/index.php/ijrcs

ASCEE

Monte Carlo Simulations on 2D LRF Based People Tracking using Interactive Multiple Model Probabilistic Data Association Filter Tracker

Zulkarnain Zainudin [a,1,*], Sarath Kodagoda [b,2]

[a] Faculty of Electronics and Computer Engineering Technology, Universiti Teknikal Malaysia Melaka (UTeM), Hang Tuah Jaya, 76100 Durian Tunggal, Melaka, Malaysia
[b] Centre for Autonomous Systems (CAS), Faculty of Engineering and Information Technology, University of Technology Sydney, PO Box 123 Broadway, Ultimo, NSW 2007, Australia
[1] zul@utem.edu.my; [2] Sarath.Kodagoda@uts.edu.au
[*] Corresponding Author

ARTICLE INFO

Article History
Received January 16, 2023
Revised February 15 2023
Accepted February 26, 2023

Keywords
People Tracking;
Interactive Multiple Model;
Support Vector Machine;
Human Robot Interaction;
Laser Range Finder

ABSTRACT

Consistency of tracking filter such as Interactive Multiple Model Probabilistic Data Association Filter (IMMPDAF) is the most important factor in targets tracking. Inaccurate tracking capability will lead to poor tracking performance when dealing with multiple people's interactions and occlusions. In order to validate the consistency, Normalized Estimation Error Squared (NEES) and Normalized Innovation Squared (NIS) were evaluated and tested using Monte Carlo experiments for 50 runs. These simulations has proven that the tracker is conditionally consistent on targets tracking despite the fact that it has difficulties on handling occlusions and maneuvering people. NEES requires ground truth of tracking data and predicted data, whereas NIS requires observation and predicted data for Monte Carlo simulations. In NEES simulations, the result emphasizes that state estimation errors of IMMPDAF tracker are inconsistent with filter-calculated covariances especially when dealing with sudden turns in zig-zag motion where quite a large number of points fall outside 95% probability region. In NIS simulations, IMMPDAF tracker is confirmed to have difficulties to handle multiple targets with a short period of occlusion although a small number of points falls outside of 95% probability region. Filter tracker is considered mismatched when dealing with zig-zag motion; however, it deemed to be optimistic when dealing with occlusions. As a result, the IMMPDAF tracker has limited capability in monitoring sharp turns under occlusion conditions, although it is acceptable when dealing with occlusions only.

1. Introduction

Automation system and robotic technology have been gradually replacing tasks of human being in the field manufacturing, security, surveillance and human robot interaction (HRI). Detecting and tracking people is one of the critical and crucial aspects in the those fields. There have been many researches and interests in populated surroundings using multiple sensors such as light detection and ranging (LiDAR) or laser range finder (LRF) [1] and camera with diversified detection and tracking techniques [2].

Several techniques and sensory modalities were employed to perform these tasks. Computer vision approaches have mostly been used, depending on the type of camera used: monocular, stereo, or RGB-Depth. Deep learning approaches provide accurate person detection in this domain. Depth information is also considered in other approaches. For example, a social robot detects humans using a Kinect sensor that combines colour and depth information [3], [4]. Skeleton-based techniques for recognising person pose and some activities or behaviours have been developed in conjunction with RGB-Depth sensors [5]. This task has also been addressed using stereo vision. Color and depth information provided by stereoscopic vision, for example, has been utilised to suggest fuzzy algorithms for recognising and tracking persons.

Despite advances in computer vision algorithms for people recognition and tracking, LiDARs are still present in the sensory systems of many mobile robots, particularly social and service robots. LiDARs are still an intriguing sensor for people detection because to their wide fields of view, excellent accuracy and robustness. Vision-only techniques, on the other hand, have significant limitations. Vision-based devices, such as monocular, stereo cameras, and RGB-Depth sensors, typically have a restricted field of view, and light conditions can have a significant impact. Deep information, in particular, is not always dependable, and false positives can occur in skeleton-based approaches.

Thus, various type of LiDARs or LRFs are still being used in high performance applications such as 3D or multichannel LiDAR by many researchers [6]. However, these kind of LiDARs are quite expensive since they are mainly used for autonomous vehicle application [7, 8, 9]. Thus, 2D LiDAR or LRF is less expensive than 3D LiDAR and preferred to be use in domestic applications [10, 11, 12, 13, 14, 15].

Several techniques have been proposed on using laser range finder as one of observation devices such as heuristic approach, motion-based and feature-based [16, 17, 18, 19, 20]. In this paper, it is opted to use feature-based and proposed the detection on a torso of a person which has a general cross-section of an ellipse.

Characteristically, laser-based tracking is faster to process data and insensitive to lighting conditions [21], [22]. It can provide a good accuracy in sparsely populated environment. However, when dealing with many interactions and occlusions of multiple people, the tracking accuracy becomes poor. To overcome this drawback, tracking on multiple people has been implemented using Bayesian filters with data association such as Joint Probabilistic Data Association Filter (JPDAF) for effective tracking [23, 24, 25, 26]. However, multiple-model-based approach in which different models run in parallel and able to describe different aspects of human models such as Interactive Multiple Model (IMM) estimator [27] is an effective methodology to deal with manoeuvring targets (people).

In general, problem on detecting people is handled using learning algorithms such as Support Vector Machines (SVM) [28], [29]. Then, the detected target is then tracked by Interactive Multiple Model (IMM) which has a constant velocity and constant turn rate models [30], [31].

As a result, measuring the performance of a state estimator for target tracking is critical, particularly when dealing with several people's interactions and occlusions. Normalized Estimation Error Squared (NEES) and Normalized Innovation Squared (NIS) are useful techniques to measure the consistency of the filter [24]. NEES requires ground truth of the tracking data and predicted data which should be applied using Monte Carlo simulations or runs. NIS is the difference between actual and predicted observation. These will aid in identifying the specific target scenarios in which the tracker excels.

This paper is organized as follows. Section 2 briefly explain features classification with regard to people detection plus tracking people algorithm using Interactive Multiple Model Probabilistic Data Association Filter (IMMPDAF). Section 3 presents the results on measurement of simulated and experimental data. Section 4 concludes the paper with contribution to the future research.

2. People Detection and Tracking

The method for detecting people is based on two dimensional (2D) laser range finder data in polar coordinates that were taken at torso height of human as shown in Fig. 1 which comprises of extracting significant features followed by a classification process. People tracking are classified into motion models and simultaneously, track management is implemented to deal with disappearing and appearing of targets due to occlusions. This process can be clearly visualised in Fig. 2.

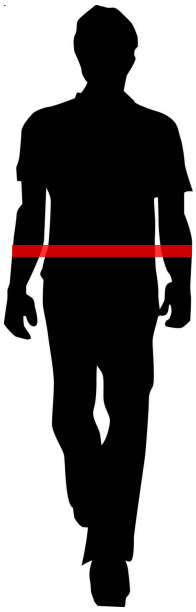

Fig. 1. Laser data taken at torso height as shown on red marking.

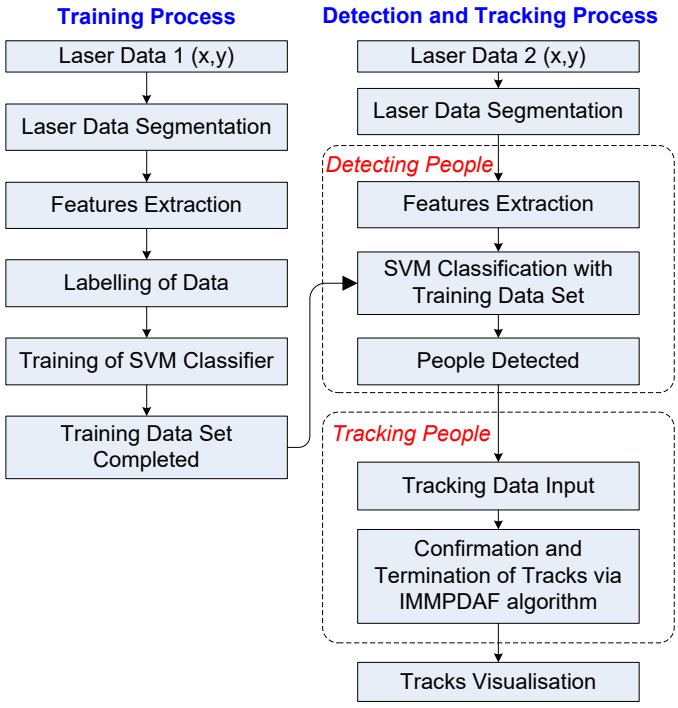

Fig. 2. The process flow on detection and tracking.

2.1. Features and Classifications

The first processing step on laser data is segmentation of data to separately recognize objects on the scan. This is based on a detection on range discontinuities in the laser scan. The laser range finder provides range and bearing, $\{r_i, \theta_i\}$ to objects in its field of view, where, suffix i refers to a specific range/bearing data with $i = 1, ..., n$. By using a model based technique, which is realized using the Extended Kalman Filter (EKF) [32, 33, 34], it is possible to partition the data into segments, $S = \{s_1, s_2, ..., s_M\}$ as shown in Fig. 3. M is the number of segment in a particular laser range/bearing data which is shown as blue dots . Symbol $'o'$ in red colour refers to discontinuity points, which define start and end points of segments.

Once the data segmentation is carried out, the succeeding step is to extract 4 features as it is subsequently used for classification process on detecting people [35]. One of the important features is implementation of ellipse fitting [36] on segmented laser data since cross section of torso of human can possibly be estimated by an ellipse as shown in red colour in Fig. 4. From this feature, the centre point of ellipse is then used for tracking purpose. Along with the four features that are extracted, a classification using radial basis function SVM (RBFSVM) is implemented [37, 38, 39].

Although the elliptical fitting technique performed admirably in general, it had significant issues with segmented data relating to occluded cases. This issue is visually explained in Fig. 5. From curves (a) through (d), ellipse fitting in red colour was done quite well, as indicated in the figure (d).

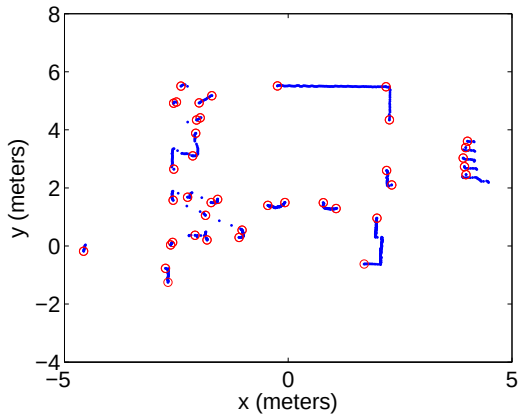

Fig. 3. Segmentation of laser data using EKF.

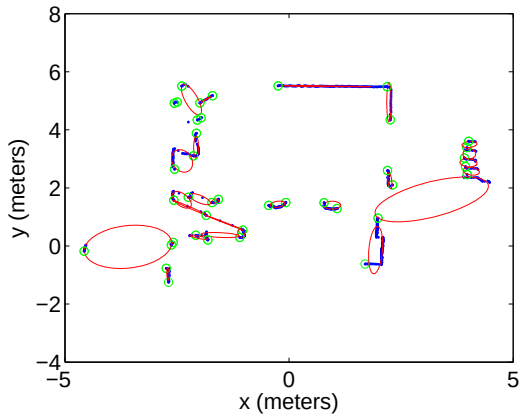

Fig. 4. Segmentation of laser data with ellipse fitting

The issue began at (e), when occlusions had caused one of the ellipses to shift significantly in size and shape. Due to the occlusions in (f), one ellipse totally vanished and began to reappear in (g). In (h), both ellipses were clearly visible when occlusions had passed.

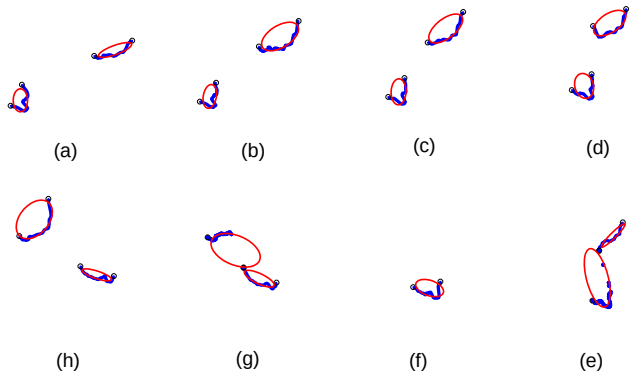

Fig. 5. Occlusion of two people

Clearly, this phenomenon can be further understood by referring to Fig. 6 and Fig. 7. The blue colour represents background objects such as wall, tables, chairs and furnitures in the vicinity of LiDAR. The red curves are representing motion of people. The occlusion occurs in the grey circle area where the shape of torso on detected people are not representing the appropriate shape of people. Therefore, this process leads a detector to have difficulties on handling the targets where disappearance and re-appearance of the targets occurs.

2.2. People Tracking Using Interacting Multiple Model (IMM) Probabilistic Data Association Filter (PDAF) Tracker

Once people were detected based on the laser data and they were monitored in real time using an Interactive Multiple Model (IMM) tracker [40], [41]. A person's mobility patterns are divided into three categories. The first model is a constant velocity model, in which the person goes ahead at a nearly constant speed in a nearly straight line. The second and third models are constant turn rate models in which the person turns at a specific angle to the left and right. It will certainly cause false detection due to the vast scatters present in the environment regarding numerous elements such

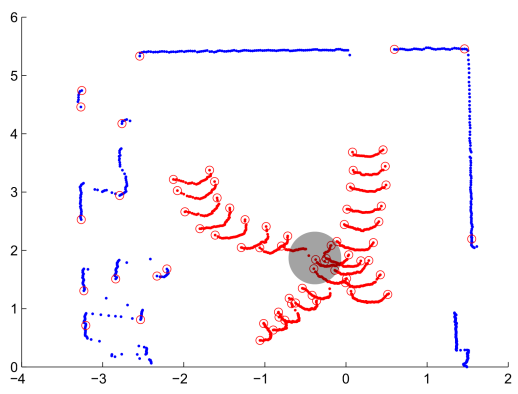

Fig. 6. Detection on two people with occlusion.

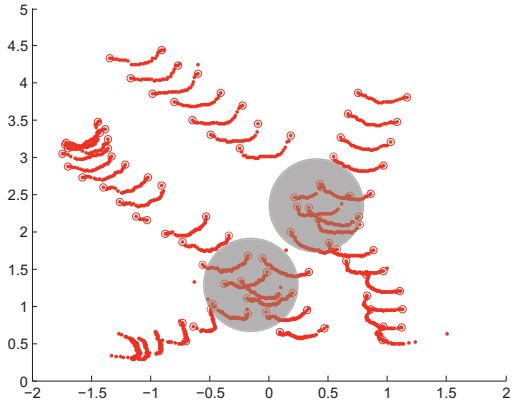

Fig. 7. Detection on three people with occlusions.

as furniture, glasses or mirrors, and metallic parts. Because the target vanished, reappeared, and navigated through the clutter, the tracking issue was intricate and difficult to solve. IMMPDAF filter with track confirmation and deletion based on criteria that met the conditions was used to solve this problem.

2.3. Track Management

Using the Markov relationship, the probability of existence of a true person $P_T(k+1|k)$ before the receiving data in scan $k+1$ is given by,

$$P_T(k+1|k) = P_{22}P_T(k|k) + P_{12}(k|k) \tag{1}$$

where P_{22} is the transition probability form an observable to observable state, and P_{12} is the transition probability from an observable to observable state. Then, probability update of person existence is

$$P_T(k+1|k+1) = \frac{1-\delta_{k+1}}{1-\delta_{k+1}P_T(k+1)}P_T(k+1|k) \tag{2}$$

where

$$\delta_{k+1} = \begin{cases} P_D P_G, & (N_{k+1}=0) \\ P_D P_G \left[1 - \overline{V}\sum_{i=1}^{N_{k+1}} \frac{1}{P_G(2\pi)^{M/2}\sqrt{S|k+1|}} e^{-d_i^2/2}\right], & (\text{otherwise}) \end{cases}$$

and $V = V_{G_{k+1}}/(N_{k+1} - P_D P_G P_T(k+1|k))$, P_D is the probability of detection, P_G is the gate probability, V_G is the gate volume, N_{k+1} is the number of measurements inside the validation gate, S is the innovation covariance, and d_i^2 is the normalized innovation squared of the ith measurement.

The log-likelihood ratio (LLR) is defined as

$$LLR_{k+1} = \ln\left(\frac{P_T}{1-P_T}\right). \tag{3}$$

Once the LLR is obtained, confirmation and termination of track thresholds are determined as

$$\begin{cases} LLR_{k+1} \geq \ln\left(\frac{1-\beta_T}{\alpha_T}\right), & (\text{declare track confirmation}) \\ \ln\left(\frac{\beta_T}{1-\alpha_T}\right) < LLR_{k+1} < \ln\left(\frac{1-\beta_T}{\alpha_T}\right), & (\text{continue test}) \\ LLR_{k+1} \leq \ln\left(\frac{\beta_T}{1-\alpha_T}\right), & (\text{delete track}) \end{cases}$$

where α_T and β_T are the probability of false-track confirmation and the probability of true-track termination, respectively.

3. Simulation and Experimental Results

3.1. Simulation Results

A simulation study has been performed to analyze the robustness and consistency of IMMPDAF tracker in tracking moving people. The sensor used is capable of detecting object up to 30 meters range. The observation is assumed to be static. There are three models considered: Model 1 refers to constant velocity with $\omega = 0$; Model 2 refers to right turn with $\omega = 1.4 rad/s$ and Model 3 refers to left turn with $\omega = -1.4 rad/s$. The mode transition-probability matrix used for the simulation **T** is

$$\begin{bmatrix} 0.95 & 0.025 & 0.025 \\ 0.025 & 0.95 & 0.025 \\ 0.025 & 0.025 & 0.95 \end{bmatrix}.$$

The algorithm performance of IMMPDAF tracker is evaluated by Monte Carlo experiments for 50 runs with random error with variance Q = diag(10,10). It is also known as "chi-square" test. A simulation of two people with a maneuvering movement in opposite direction and having an occlusion on the first track shown in Fig. 8. Targets are assumed to be detected correctly.

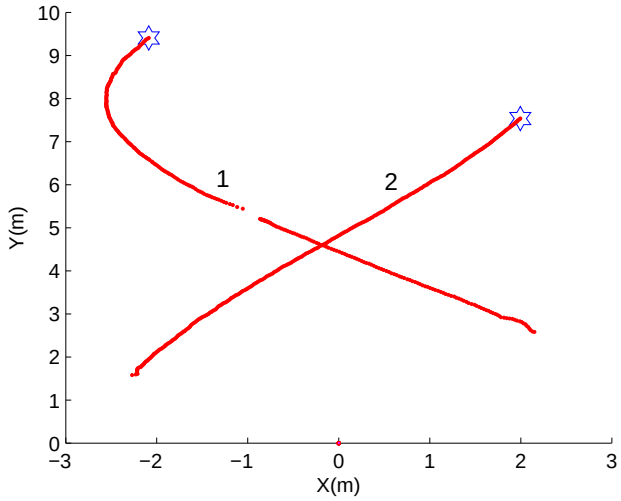

Fig. 8. Tracking of two people with occlusion

The result of Normalized Estimation Error Squared (NEES) and RMS error on both x and y axes are presented to provide a consistency check for filter divergence. The NEES is obtained from the innovation or residual and the innovations covariance at each k-time. The innovation is the difference between the measurement and its prediction at time k is

$$\tilde{x}(k|k) = \mathbf{x}(k|k) - \tilde{x}(k|k-1) \tag{4}$$

The innovations covariance matrix $S(k|k)$ is given by

$$S(k|k) = \mathbf{H}(k|k)P(k|k-1)\mathbf{H}(k|k)' + \mathbf{R} \tag{5}$$

NEES is calculated as the following equation:

$$\text{NEES} = \tilde{x}(k|k)'S(k|k)^{-1}\tilde{x}(k|k) \tag{6}$$

where $\tilde{x}(k|k) = x(k) - \hat{x}(k|k)$, $x(k)$ is the true position and $\hat{x}(k|k)$ is the predicted position by the tracker in the k-th time. $P(k|k-1)$ and **R** are the predicted target state and measurement covariance matrices respectively.

RMS Error is defined as the following equation:

$$\text{RMS Error} = \sqrt{\frac{\sum_{k=1}^{n} \left(x(k|k) - \hat{x}(k|k-1)\right)^2}{n}}. \tag{7}$$

According to Bar-Shalom's book [30] as it is specifically mentioned on the pages 83 and from 234 to 236, the 95% probability region for χ_2^2 can be taken as two-sided probability region (cutting off both 2.5% tails) as the lower and upper limit of the two sided 95% region are 0.05 and 7.38 respectively. The upper limit is of the interest since the lower limit is practically near zero. In the track 1, as shown in Fig. 9, the values of NEES are found to be outside of 95% probability region when the occlusion occurs at time frame between 110 and 120. The time difference between two frames is 0.2 second. On the other hand, in the track 2 as shown in Fig. 10, the values of NEES is within the 95% probability region which means the IMM state estimation is consistent.

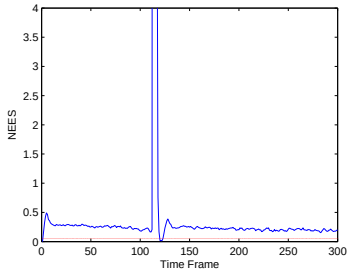

Fig. 9. NEES of track 1 of two people with occlusion

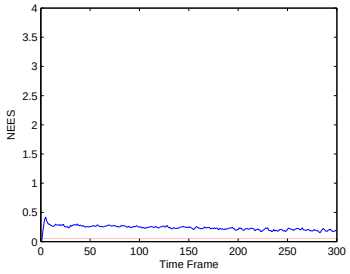

Fig. 10. NEES of track 2 of two people with occlusion

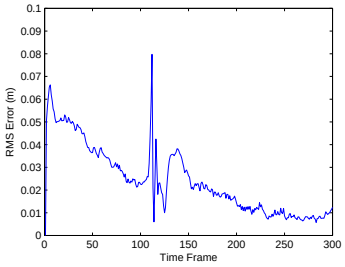

Fig. 11. X_{rms} error for track 1

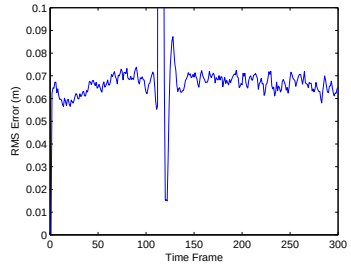

Fig. 12. Y_{rms} error for track 1

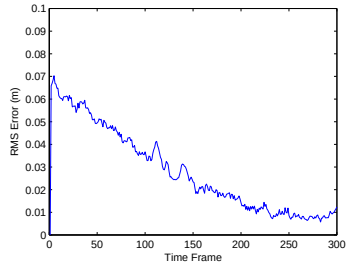

Fig. 13. X_{rms} error for track 2

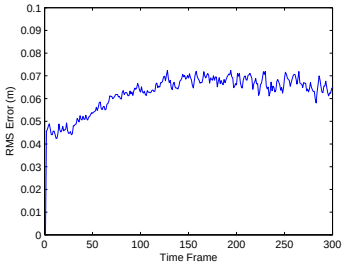

Fig. 14. Y_{rms} error for track 2

For RMS error for 50 Monte carlo runs in x and y axes for track 1 and track 2 respectively are shown in Fig. 11-14, the value of RMS error is consistently small except sudden change when the occlusion occurs at time frame between 110 and 120. This figure shows a prove that the tracking performance is good for IMMPDAF except at the sudden change time frame.

The simulation on a person as shown in Fig. 15 that moves in a circular motion carried out to get the pose of human torso from various angle as its observation point is at coordinate (0,0). Ground truth and predicted points are shown in blue dots and red dots respectively. The person is assumed to move in a constant velocity with constant turn rate. The value of NEES for 50 Monte Carlo runs is within the lower and upper limit of the two-sided of 95% region as referred to Fig. 17.

Further analyses on simulated motion of 2 people with a zig-zag and a curve motion are shown in Fig. 16. Ground truth and predicted points are shown in blue dots and red dots respectively. The values of NEES on track 1 for 50 Monte Carlo runs in a zig-zag motion are outside of the lower limit and upper limit of the two-sided of 95% region on time frame 70 to 80 as shown in Fig. 18. Similarly as shown in Fig. 19, the values of NEES on track 2 that are outside of the 95% region can be seen

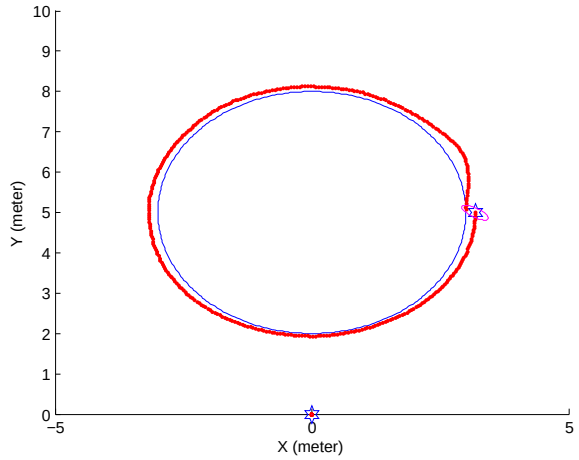

Fig. 15. Tracking on human pose from various angles in a circular motion

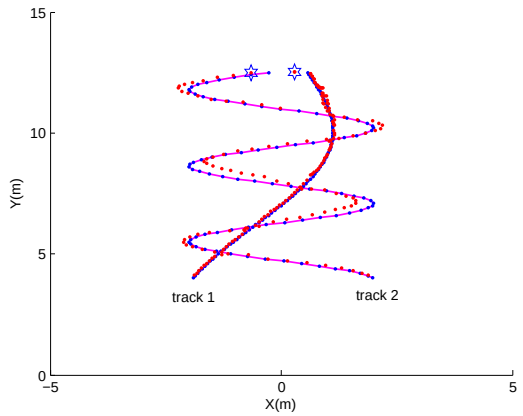

Fig. 16. Tracking of 2 people in a zig-zag and curve motion

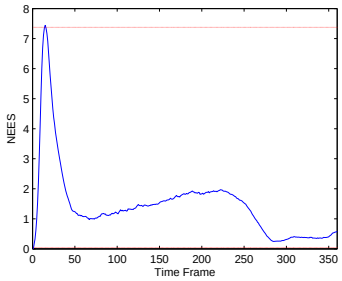

Fig. 17. NEES of a person in a circular motion

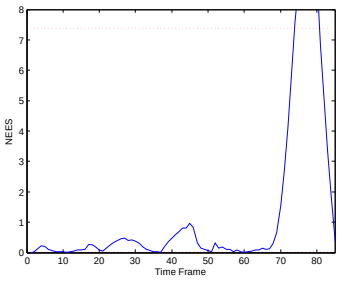

Fig. 18. NEES of track 1 in a zig-zag motion

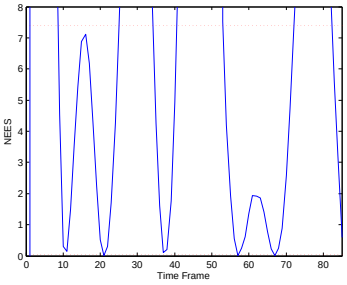

Fig. 19. NEES of track 2 in a curve motion

on multiple time frames 1 to 9, 25 to 34, 41 to 53 and 72 to 82. This mismatch caused 39 points out of 85 to outside the 95% probability region. The errors are too large compared to filter-calculated covariance. This result shows a prove that IMMPDAF has difficulties on handling sudden turns in the track 2 with zig-zag motion and this filter is said to be mismatched filter and clearly an unacceptable situation.

From this observation, it can be seen that the result on tracking performance on this simulation emphasizes that state estimation errors of IMMPDAF tracker are inconsistent with the filter-calculated covariances.

3.2. Occlusion Handling with Probabilistic Data Association Filter (PDAF)

Fig. 20 shows tracking of two people (T1 and T2) using a stationary observer. T1 and T2's motions resulted in an occlusion, in which T1 was temporarily removed from observations. The track could be re-associated with T1 for further tracking due to the IMM tracker's predictions. Due to the nature of tracking ability based on the observation of laser tracking data, its visual representation was not precise.

Fig. 21 shows the results of tracking on two people by using a dynamic observer. The occlusion induced by T1 and T2's motions caused T2 to temporarily disappear from the view, and the scenario is very similar to that of the stationary observer. Due to the same difficulty as with the stationary observation, the visual representation of tracking is not accurate. Due to the effect of faulty observation data, the track T2 is skewed to the left side of the original track, and the other track T1 is terminated. T2 will reappear as a new target if it has the potential to be terminated after it is missing for an extended period of time.

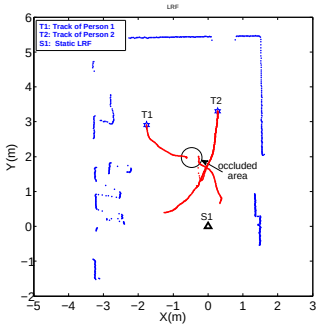

Fig. 20. People tracking results: with a stationary observer. T1 and T2 denote the tracked of two persons

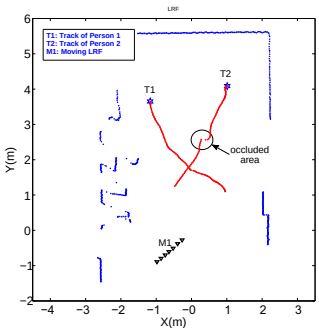

Fig. 21. People tracking results: with a moving observer. T1 and T2 denote the tracked of two persons

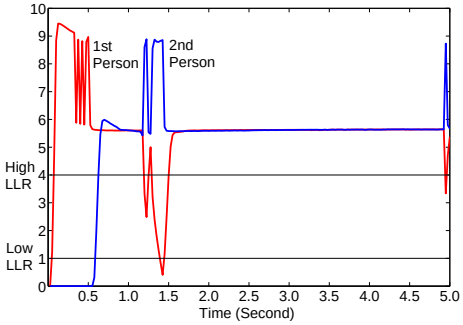

Fig. 22. The log-likelihood ratio (LLR) of two targets tracking

The log-likelihood ratio is used in the track determination process (LLR) which is shown in Fig. 22. 1st person or red line is representing track T1 and 2nd person or blue line represents track T2 as it is shown in Fig. 20. If the LLR is higher than an upper threshold, a new track is confirmed, and if it falls below a lower level, a track is deleted. Refer to track T2 or red line, when the time is between 0 and 1 second, it has higher value of LLR which is above the high LLR threshold and the track is confirmed; and when the time is between 1 and 1.4 seconds, its value is lower than the low LLR threshold and the track is deleted. Then, when the time is between 1.4 and 1.6, its LLR value reaches more than the high LLR threshold, it has reconfirmed as a new track.

If the tracks are occluded for a long time and meet the LLR criteria, they may be removed and re-appear as new tracks. This is acceptable if the application does not really require the identification and tracking of a specific person. Thus, if it is necessary to identify and track the target, temporal prediction on tracking is needed to be implemented which it can hold the tracks and does not register as new targets.

3.3. Experimental Results

The platform used in our experiments is a Segway robot equipped with laser range finder and computer as shown in Fig. 23. It has an onboard computer, AMD Athlon II X2 255, Dual Core, 3.1 GHz with 4GB DDR3 running on Linux Ubuntu 9.10 operating system. This system uses a HOKUYO UTM-30LX laser range finder that has 30 meters of detection range, 0.25^o angular resolution, 270^o of angular field of view and 25 milliseconds sampling period. The Segway robot is used in a stationary position to horizontally monitor the environment. The experiments were conducted in a common area of CAS.

Experiments was conducted on tracking three people that are carried out in 190 scans in a common area of the faculty as shown in Fig. 24. The segway robot is used in stationary position to monitor the environment. To evaluate the performance of this tracker, we present the results of Normalized Innovation Squared (NIS) [30]. The equation of NIS is

$$\text{NIS} = \tilde{x}(k|k)' S(k|k)^{-1} \tilde{x}(k|k) \tag{8}$$

where $\tilde{x}(k|k) = x(k) - \hat{x}(k|k)$, $x(k)$ is the position from the sensor measurements and $\hat{x}(k|k)$ is the predicted position by the tracker in the k-th time.

From this experiment, there are two occlusions where the tracks lost for a short period: track 1 at time frame of 100 to 115 and track 2 at time frame 120 to 140 as shown in Fig. 25 and Fig. 26. At the occlusions time frame, it seems that the tracks are not accurately visualised and they are slightly

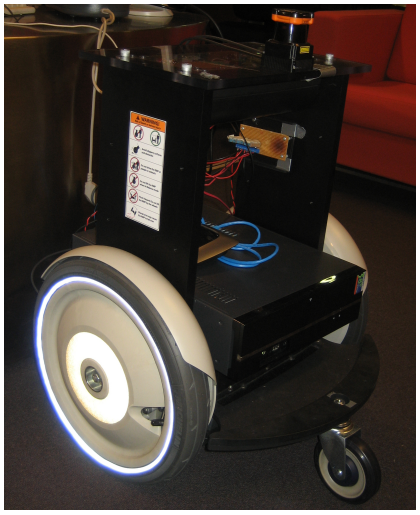

Fig. 23. Robot used for the experiment

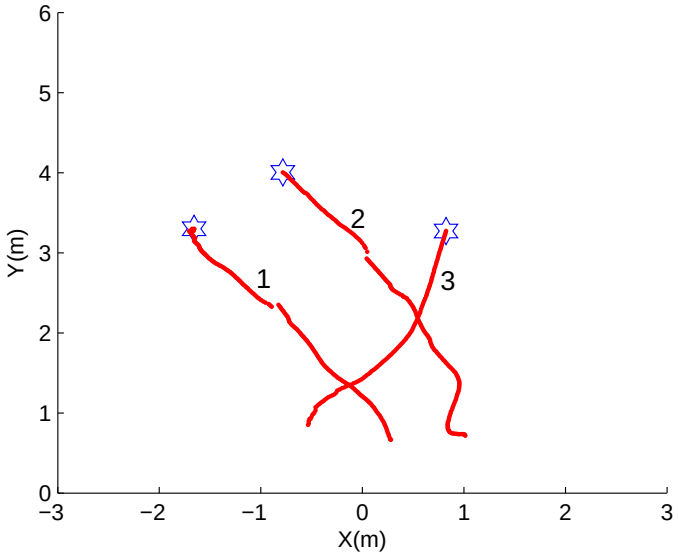

Fig. 24. Tracking on 3 people with occlusions

skewed from the original tracks. In track 1 and 2, less than 20 points out of 180 points falls outside the 95% region which is acceptable. This tracker is said to optimistic. In track 3 as shown in Fig. 27, there is no occlusion occurs and thus the value of NIS within the upper and lower limit.

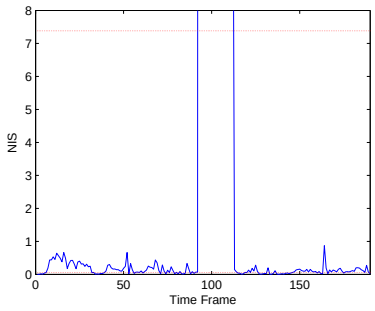

Fig. 25. NIS of track 1

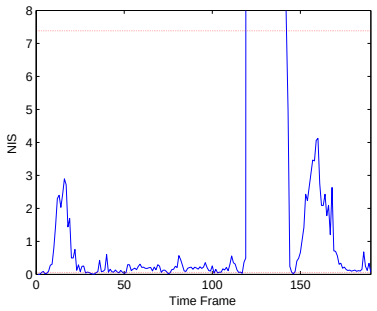

Fig. 26. NIS of track 2

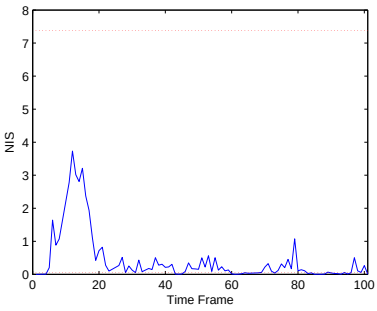

Fig. 27. NIS of track 3

For overall performance, NIS values for three tracks are fall within 95% probability region except when the occlusions occur. Hence, it is proved that the tracker is conditionally consistent. However, it is confirmed that the current tracker has difficulties to handle multiple targets with a long period of occlusion.

4. Conclusion and Future Work

This paper described a system for tracking people that employs a 2D laser range finder as a sensor at torso height. With poor accuracy, the IMMPDAF tracker was partially incapable of monitoring sharp manoeuvring human movements under occlusion scenarios. The results of simulated data have proven that the existing tracking approach has issues dealing with occlusions and zig-zag motion with NEES values that surpass the upper bound. As a result, the filter tracker is considered mismatched. Based on the experimental data, NIS of the current tracker has produced some points that exceed the 95% probability region, thus this filter is deemed to be optimistic and this tracker is acceptable despite the problems in dealing with occlusions. In current work, 3 models with constant velocity, turn left and right have already been implemented with some drawbacks that has been discussed and shown

through simulation and experimental analyses. As a result, the findings of these analyses will make for fascinating future research. In future, the work will focus on methodology to improve temporal prediction of multiple targets with optimization of training data.

Author Contribution: All authors contributed equally to the main contributor to this paper. All authors read and approved the final paper.

Funding: This research received no external funding.

Acknowledgment: This work is supported by the Centre of Autonomous Systems (CAS), University of Technology, Sydney, Australia; Centre for Telecommunication Research and Innovation (CeTRI), Universiti Teknikal Malaysia Melaka (UTeM), Malaysia and the Ministry of Higher Education (MoHE), Malaysia.

Conflicts of Interest: The authors declare no conflict of interest.

References

[1] L. Beyer, A. Hermans, T. Linder, K. O. Arras, and B. Leibe, "Deep person detection in two-dimensional range data," *IEEE Robotics and Automation Letters*, vol. 3, pp. 2726–2733, 2018, https://doi.org/10.1109/LRA.2018.2835510.

[2] K. Koide, J. Miura, and E. Menegatti, "Monocular person tracking and identification with online deep feature selection for person following robots," *Robotics and Autonomous Systems*, vol. 124, p. 103348, 2020, https://doi.org/10.1016/j.robot.2019.103348.

[3] A. Ramey, Álvaro Castro-González, M. Malfaz, F. Alonso-Martin, and M. A. Salichs, "Vision-based people detection using depth information for social robots," *International Journal of Advanced Robotic Systems*, vol. 14, p. 415–428, 2017, http://doi.org/10.1177/1729881417705923.

[4] G. T. Papadopoulos, A. Axenopoulos, and P. Daras, "Real-time skeleton-tracking-based human action recognition using kinect data," in *International Conference on Multimedia Modeling*, 2014, pp. 473–483, http://doi.org/10.1007/978-3-319-04114-8_40.

[5] A. M. Ahmad, Z. Bazzal, and H. A. Youssef, "Kinect-based moving human tracking system with obstacle avoidance," *Advances in Science, Technology and Engineering Systems Journal*, vol. 2, pp. 191–197, 2017, http://doi.org/10.25046/aj020325.

[6] A. Borcs, B. Nagy, and C. Benedek, "Instant object detection in lidar point clouds," *IEEE Geoscience and Remote Sensing Letters*, vol. 14, no. 7, pp. 992–996, 2017, https://doi.org/10.1109/LGRS.2017.2674799.

[7] Z. Dai, A. Wolf, P. Ley, T. Glück, M. C. Sundermeier, and R. Lachmayer, "Requirements for automotive lidar systems," *Sensors*, vol. 22, no. 19, p. 7532, 2022, https://doi.org/10.3390/s22197532.

[8] M. E. Warren, "Automotive lidar technology," in *2019 Symposium on VLSI Circuits*, 2019, pp. C254–C255, https://doi.org/10.23919/vlsic.2019.8777993.

[9] Y. Li and J. Ibañez-Guzmán, "Lidar for autonomous driving: The principles, challenges, and trends for automotive lidar and perception systems," *IEEE Signal Process. Mag.*, vol. 37, no. 4, pp. 50–61, 2020, https://doi.org/10.1109/MSP.2020.2973615.

[10] J. Shackleton, B. VanVoorst, and J. Hesch, "Tracking people with a 360-degree lidar," in *2010 7th IEEE International Conference on Advanced Video and Signal Based Surveillance*, 2010, pp. 420–426, https://doi.org/10.1109/AVSS.2010.52.

[11] A. H. A. Rahman, K. A. Z. Ariffin, N. S. Sani, and H. Zamzuri, "Pedestrian detection using triple laser range finders," *International Journal of Electrical & Computer Engineering*, vol. 7, no. 6, 2017, http://doi.org/10.11591/ijece.v7i6.pp3037-3045.

[12] J. Chen, P. Ye, and Z. Sun, "Pedestrian detection and tracking based on 2d lidar," *The 2019 6th International Conference on Systems and Informatics (ICSAI 2019)*, pp. 421–426, 2019, https://doi.org/10.1109/ICSAI48974.2019.9010202.

[13] H. Beomsoo, A. A. Ravankar, and T. Emaru, "Mobile robot navigation based on deep reinforcement learning with 2d-lidar sensor using stochastic approach," in *2021 IEEE International Conference on Intelligence and Safety for Robotics (ISR)*, 2021, https://doi.org/10.1109/ISR50024.2021.9419565.

[14] H. Beomsoo, A. A. Ravankar, and T. Emaru, "Mobile robot navigation based on deep reinforcement learning with range only sensor," in *The Proceedings of JSME annual Conference on Robotics and Mechatronics (Robomec)*, vol. 2021, 2021, pp. 1P1–L07, https://doi.org/10.1299/jsmermd.2021.1P1-L07.

[15] D. L. Tomasi and E. Todt, "Cbnav: Costmap based approach to deep reinforcement learning mobile robot navigation," in *2021 Latin American Robotics Symposium (LARS), 2021 Brazilian Symposium on Robotics (SBR), and 2021 Workshop on Robotics in Education (WRE)*, 2021, https://doi.org/10.1109/LARS/SBR/WRE54079.2021.9605463.

[16] Z. Zhang and K. Kodagoda, "Multi-sensor approach for people detection," in *Proceedings of the 2005 International Conference on Intelligent Sensors, Sensor Networks and Information Processing Conference*, 2005, pp. 355–360, https://doi.org/10.1109/ISSNIP.2005.1595605.

[17] Z. Zivkovic and B. Krose, "Part based people detection using 2d range data and images," in *2007 IEEE/RSJ International Conference on Intelligent Robots and Systems*, 2007, pp. 214–219, https://doi.org/10.1109/IROS.2007.4399311.

[18] O. Mozos, R. Kurazume, and T. Hasegawa, "Multi-part people detection using 2d range data," *International Journal of Social Robotics*, vol. 2, pp. 31–40, 2010, https://doi.org/10.1007/s12369-009-0041-3.

[19] K. Arras, O. Mozos, and W. Burgard, "Using boosted features for the detection of people in 2d range data," in *Proceedings 2007 IEEE International Conference on Robotics and Automation*, 2007, pp. 3402–3407, https://doi.org/10.1109/ROBOT.2007.363998.

[20] Y. Nakamori, Y. Hiroi, and A. Ito, "Multiple player detection and tracking method using a laser range finder for a robot that plays with human," *ROBOMECH Journal*, vol. 5, no. 1, pp. 1–15, 2018, https://doi.org/10.1186/s40648-018-0122-x.

[21] M. Simpson and D. Hutchinson, "Imaging — lidar," in *Encyclopedia of Modern Optics*, R. D. Guenther, Ed. Oxford: Elsevier, 2005, pp. 169–178, https://doi.org/10.1016/B0-12-369395-0/00720-X.

[22] P. Dong and Q. Chen, *LiDAR Remote Sensing and Applications*. CRC Press, 2018, https://doi.org/10.4324/9781351233354.

[23] H. A. Blom and Y. Bar-Shalom, "The interacting multiple model algorithm for systems with markovian switching coefficients," *Automatic Control, IEEE Transactions on*, vol. 33, no. 8, pp. 780–783, 1988, https://doi.org/10.1109/9.1299.

[24] Y. Bar-Shalom, T. E. Fortmann, and P. G. Cable, "Tracking and data association," *The Journal of the Acoustical Society of America*, vol. 87, p. 918, 1990, https://doi.org/10.1121/1.398863.

[25] Y. Bar-Shalom, K. Chang, and H. A. Blom, "Tracking of splitting targets in clutter using an interacting multiple model joint probabilistic data association filter," in *[1991] Proceedings of the 30th IEEE Conference on Decision and Control*, 1991, pp. 2043–2048, https://doi.org/10.1109/CDC.1991.261778.

[26] Y. Bar-Shalom, F. Daum, and J. Huang, "The probabilistic data association filter," *IEEE Control Systems Magazine*, vol. 29, no. 6, pp. 82–100, 2009, https://doi.org/10.1109/MCS.2009.934469.

[27] G. S. Satapathi and S. Pathipati, "Waveform agile sensing approach for tracking benchmark in the presence of ecm using immpdaf," *Radioengineering*, vol. 26, no. 1, pp. 227–239, 4 2017, https://www.radioeng.cz/fulltexts/2017/17_01_0227_0239.pdf.

[28] L. Cambuim and E. Barros, "Fpga-based pedestrian detection for collision prediction system," *Sensors*, vol. 22, no. 12, p. 4421, 2022, https://doi.org/10.3390/s22124421.

[29] Z. Chen, W. Yuan, M. Yang, C. Wang, and B. Wang, "Svm based people counting method in the corridor scene using a single-layer laser scanner," in *2016 IEEE 19th International Conference on Intelligent Transportation Systems (ITSC)*, 2016, pp. 2632–2637, https://doi.org/10.1109/ITSC.2016.7795979.

[30] Y. Bar-Shalom and X.-R. Li, *Estimation and tracking: principles, techniques, and software*. Artech House Norwood, 1993, https://books.google.com.my/books?id=0YPAAAAACAAJ.

[31] Y. Bar-Shalom, X. Li, and T. Kirubarajan, *Estimation with Applications to Tracking and Navigation: Theory, Algorithms and Software*. Wiley, 2001, https://doi.org/10.1002/0471221279.

[32] S. Bhaumik and P. Date, *The Kalman filter and the extended Kalman filter*. Chapman and Hall/CRC, 2019, ch. Book: Nonlinear Estimation, pp. 27–50, http://doi.org/10.1201/9781351012355-2.

[33] A. Roux, S. Changey, J. Weber, and J.-P. Lauffenburger, "Projectile trajectory estimation: performance analysis of an extended kalman filter and an imperfect invariant extended kalman filter," in *2021 9th International Conference on Systems and Control (ICSC)*, 2021, pp. 274–281, https://doi.org/10.1109/ICSC50472.2021.9666713.

[34] I. Ullah, X. Su, X. Zhang, and D. Choi, "Simultaneous localization and mapping based on kalman filter and extended kalman filter," *Wirel. Commun. Mob. Comput.*, vol. 2020, pp. 1–12, 2020, http://doi.org/10.1155/2020/2138643.

[35] Z. Zainudin, S. Kodagoda, and G. Dissanayake, "Torso detection and tracking using a 2d laser range finder," in *Proceedings of the Australasian Conference on Robotics and Automation*, 2010, http://hdl.handle.net/10453/16405.

[36] A. Fitzgibbon, M. Pilu, and R. B. Fisher, "Direct least square fitting of ellipses," *IEEE Transactions on Pattern Analysis and Machine Intelligence*, vol. 21, no. 5, pp. 476–480, 1999, https://doi.org/10.1109/TVT.2004.834875.

[37] K. Thurnhofer-Hemsi, E. López-Rubio, M. A. Molina-Cabello, and K. Najarian, "Radial basis function kernel optimization for support vector machine classifiers," *arXiv preprint arXiv:2007.08233*, Jul. 2020, https://doi.org/10.48550/arXiv.2007.08233.

[38] P. Dhivya and S. Vasuki, "Wavelet based mri brain image classification using radial basis function in svm," in *2018 2nd International Conference on Trends in Electronics and Informatics (ICOEI)*, 2018, https://doi.org/10.1109/ICOEI.2018.8553738.

[39] C. W. Hsu, C. C. Chang, C. J. Lin *et al.*, "A practical guide to support vector classification," 2003, https://www.csie.ntu.edu.tw/~cjlin/papers/guide/guide.pdf.

[40] B. Kovacevic, D. Ivkovic, and Z. Radosavljevic, "Immpdaf approach for l-band radar multiple target tracking," in *2020 19th International Symposium INFOTEH-JAHORINA (INFOTEH)*, 2020, pp. 1–5, https://doi.org/10.1109/INFOTEH48170.2020.9066328.

[41] K. R. S. Kodagoda, S. S. Ge, W. S. Wijesoma, and A. P. Balasuriya, "Immpdaf approach for road-boundary tracking," *IEEE Transactions on Vehicular Technology*, vol. 56, no. 2, pp. 478–486, 2007, https://doi.org/10.1109/TVT.2007.891426.